

Electronic Supplementary Material (ESI) for New Journal of Chemistry.

Effect of Indium Doping on Hydrogen Evolution Performance of g-C₃N₄ Based Photocatalysts

Xiaohang Yang,^a Zilong Guo,^b Xiaoyu Zhang,^a Yandong Han,^b Zheng Xue,^b Tengfeng Xie^a and Wensheng

Yang^{*,a,b}

^a State Key Laboratory of Inorganic Synthesis and Preparative Chemistry, College of Chemistry, Jilin University, Changchun

130012, China

^b Institute of Molecular Plus, Tianjin University, Tianjin 300072, China

E-mail: wsyang@jlu.edu.cn

Contents

1. TEM images of the pristine g-C ₃ N ₄ and In-g-C ₃ N ₄ photocatalysts.	S2
2. STEM image of the In-g-C ₃ N ₄ photocatalyst doped with 2.18 wt.% indium.	S2
3. Survey XPS spectra of the In-g-C ₃ N ₄ photocatalysts.	S3
4. High resolution C 1s and O 1s XPS spectra of the In-g-C ₃ N ₄ photocatalysts.	S3
5. H ₂ evolution over the In-g-C ₃ N ₄ photocatalyst during four cycles of the reactions	S4
6. Nitrogen adsorption-desorption isotherms of the In-g-C ₃ N ₄ photocatalysts.	S5
7. Tauc plots of the In-g-C ₃ N ₄ photocatalysts.	S6
8. Valence band XPS (VB-XPS) spectra of the In-g-C ₃ N ₄ photocatalysts.	S6
9. Photoluminescence spectra of the In-g-C ₃ N ₄ photocatalysts.	S7
10. Comparison in photocatalytic activities of g-C ₃ N ₄ photocatalysts.	S7
11. Transient emission decays of the In-g-C ₃ N ₄ photocatalysts.	S8

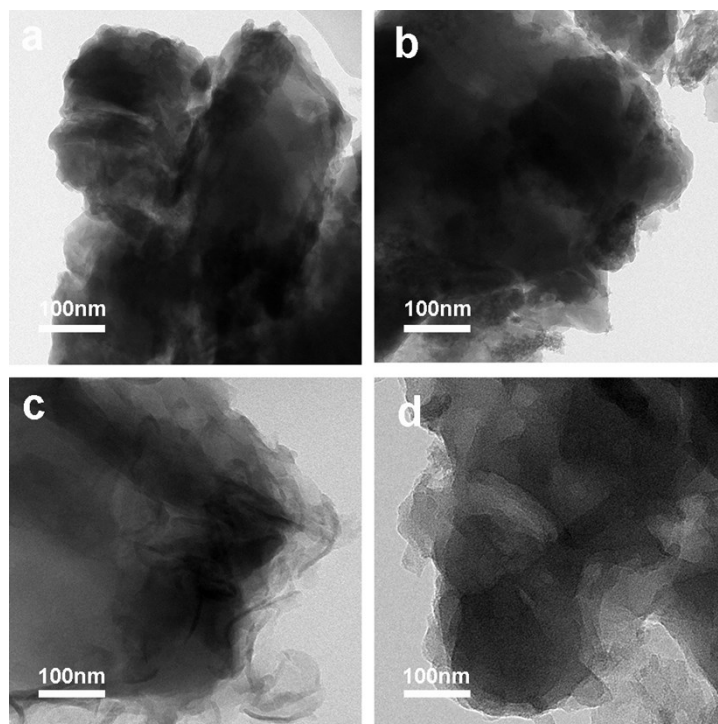


Fig. S1 TEM images of the (a) pristine g-C₃N₄ and In-g-C₃N₄ photocatalysts doped with (b) 0.52 wt.%, (c) 1.15 wt.% and (d) 2.21 wt.% indium. All the samples presented the similar sheet-like structure, meaning the doping of indium had little effect on layered structure of the g-C₃N₄.

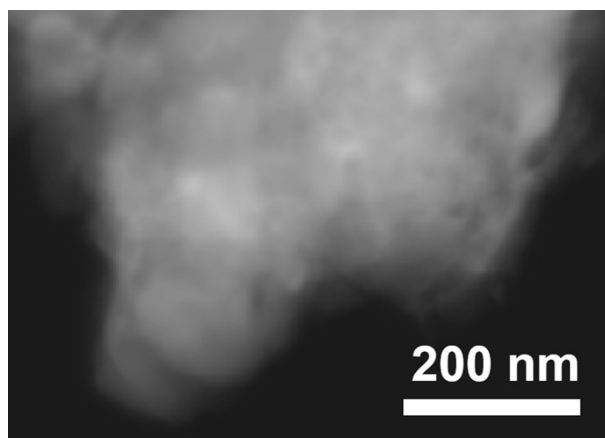


Fig. S2 High-annular dark-field scanning transmission electron microscopy (STEM) image of the In-g-C₃N₄ photocatalyst doped with 2.18 wt.% indium, corresponding to the elemental mapping images shown in Fig. 1b–e.

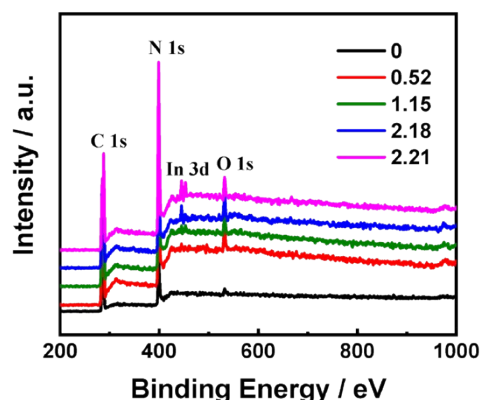


Fig. S3 Survey XPS spectra of the pristine $g\text{-C}_3\text{N}_4$ and $\text{In-g-C}_3\text{N}_4$ photocatalysts doped by 0.52, 1.15, 2.18 and 2.21 wt.% indium. Intensity of the C1s and N1s peaks kept less changed, while that of In and O gradually increased with the increased amount of In doped. The atomic ratio of O to C (O/C) increased from 3.09% to 6.76%, 7.63%, 10.34% and 12.7% when the amount of indium doped increased from 0 to 0.52, 1.15, 2.18 and 2.21 wt.%, attributed to the increased surface areas of the photocatalyst with the increased amount of In doped (see Fig. S6).

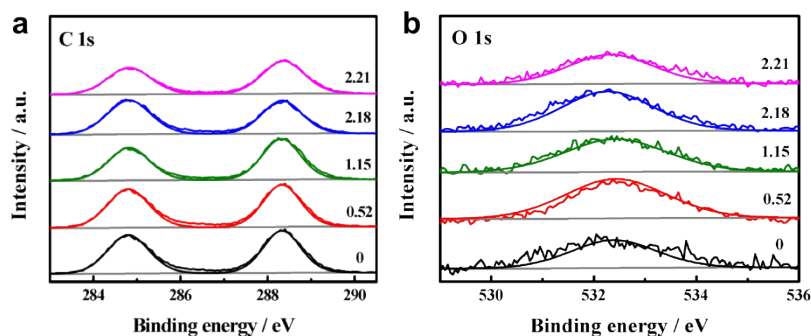


Fig. S4 High resolution XPS spectra (a) C 1s and (b) O 1s of the pristine $g\text{-C}_3\text{N}_4$ and $\text{In-g-C}_3\text{N}_4$ photocatalysts doped with 0.52, 1.15, 2.18 and 2.21 wt.% indium. The C 1s peaks at 288.4 and 284.8 eV in the pristine $g\text{-C}_3\text{N}_4$, assigned to the C-N-C and C-C groups, as well as the O 1s peak centered at 532.5 eV, ascribed to the adsorbed oxygen, experienced negligible shift upon the doping of indium, implying that there were no interactions between indium with the C and O atoms in the $\text{In-g-C}_3\text{N}_4$.

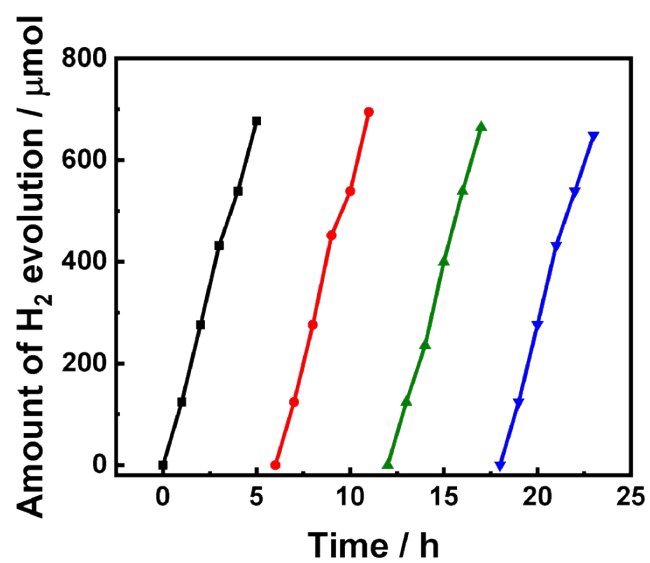


Fig. S5 Variations in H₂ evolution over the In-g-C₃N₄ photocatalyst doped with 2.18 wt.% indium during four cycles of the reactions. The almost unchanged H₂ evolution rate after the four cycles indicated the good stability of the photocatalyst.

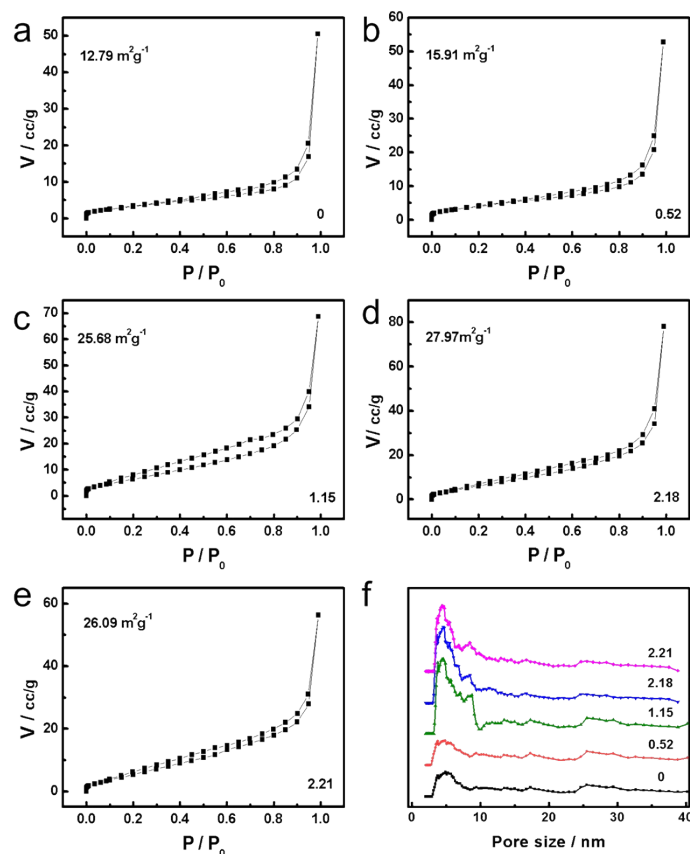


Fig. S6 Nitrogen adsorption-desorption isotherms of the In-g-C₃N₄ photocatalysts doped with (a) 0 wt.%, (b) 0.52 wt.%, (c) 1.15 wt.%, (d) 2.18 wt.% and (e) 2.21 wt.% indium and (f) the corresponding size distribution curves. Surface areas of the In-g-C₃N₄ photocatalysts were determined to be 12.79, 15.91, 25.68, 27.97 and 26.09 m²g⁻¹, and their pore volumes were 0.07, 0.08, 0.11, 0.11 and 0.08 cm³g⁻¹ when the amounts of indium doped were 0, 0.52, 1.15, 2.18 and 2.21 wt.%. According to the derived pore size distribution plots (Fig. S5f), sizes of the mesopores in the pristine g-C₃N₄ were primarily distributed in the range of 3–5 nm, while additional mesopores with sizes in the range of 8–9 nm were identified for the In doped photocatalysts. The In-g-C₃N₄ photocatalysts doped with 1.15 and 2.18 wt.% indium presented comparable surface areas (25.68 and 27.97 m²·g⁻¹) and the same pore volume (0.11 cm³·g⁻¹) but very different H₂ evolution rates (0.39 and 1.35 mmol·h⁻¹·g⁻¹), suggesting that the differences in surface area and thus the amount of surface active sites are not the primary reason responsible for the improved photocatalytic activity.

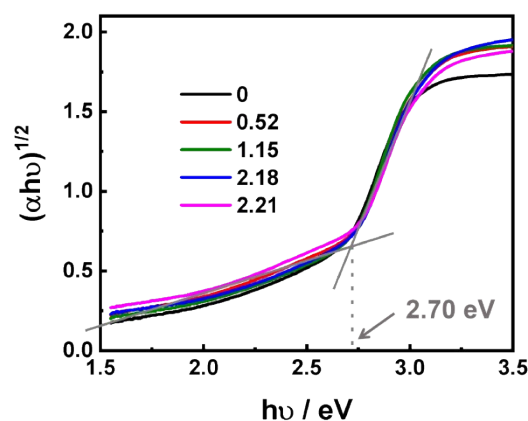


Fig. S7 Tauc plots of the In-g-C₃N₄ photocatalysts doped with 0, 0.52, 1.15, 2.18 and 2.21 wt.% indium derived from the UV-Vis spectra shown in Fig. 3b. The value reckoned from the X intercept at the tangent of Tauc plots (2.70 eV) corresponding to the band gap value (E_g) of the semiconducting g-C₃N₄, which kept almost unchanged with the increased amount of indium doped, meaning the indium doping had little effect on band structure of g-C₃N₄.

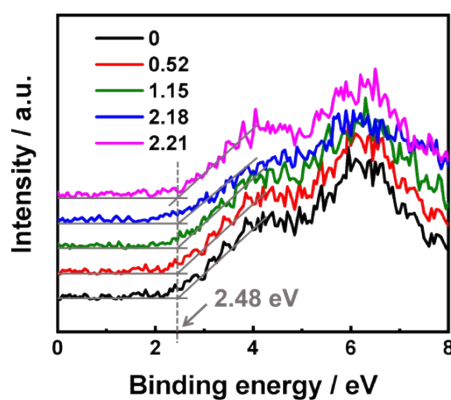


Fig. S8 Valence band XPS (VB-XPS) spectra of the In-g-C₃N₄ photocatalysts doped with 0, 0.52, 1.15, 2.18 and 2.21 wt.% indium. The valence band maximum (VBM) potential (2.48 eV) of the In-g-C₃N₄ photocatalysts kept less changed with the amount of indium doped. Combined with the appropriate E_g value (ca. 2.70 eV), the conduction band minimum (CBM) of In-g-C₃N₄ photocatalysts were calculated as -0.22 eV. Notably, In-g-C₃N₄ photocatalysts exhibited comparable energy band structure, which further elucidated that the doping of indium had little effect on forbidden band width and reducing ability of the g-C₃N₄.

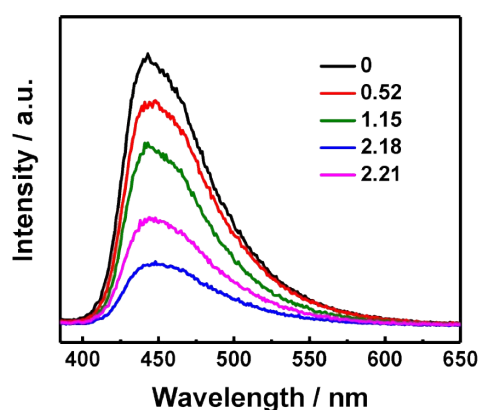


Fig. S9 Photoluminescence spectra of the In- $g\text{-C}_3\text{N}_4$ photocatalysts with 0, 0.52, 1.15, 2.18 and 2.21 wt.% of doped indium. Intensity of the emission peak of $g\text{-C}_3\text{N}_4$ at 447 nm decreased upon the doping of indium, indicating the doping of indium was effective to suppress the recombination of the photogenerated electron-hole pairs. The $g\text{-C}_3\text{N}_4$ doped with 2.18 wt.% indium presented the lowest PL emission intensity, implying optimized separation efficiency of the photogenerated charge carriers, which was in consistent with the SPV result in Fig. 4c.

Table S1 Comparison in visible light ($\lambda > 420$ nm) photocatalytic activities of the In^{3+} doped $g\text{-C}_3\text{N}_4$ with the typical transition or alkali metal ions doped $g\text{-C}_3\text{N}_4$.

Catalyst	Doped ions	H_2 evolution rate ($\text{mmol}\cdot\text{h}^{-1}\cdot\text{g}^{-1}$)	Ref.
$g\text{-C}_3\text{N}_4$	--	0.08	
$g\text{-C}_3\text{N}_4$	In^{3+} (2.18 wt.%)	1.35	This work
$g\text{-C}_3\text{N}_4$	Co^{2+} (0.46 wt.%)	0.45	Ref. 11 in the text
$g\text{-C}_3\text{N}_4$	Zn^{2+} (13.65 wt.%)	0.30	Ref. 12 in the text
$g\text{-C}_3\text{N}_4$	Mn^{2+} (2.93 wt.%)	0.13	Ref. 14 in the text
$g\text{-C}_3\text{N}_4$	Ni^{2+} (20.55 wt.%)	0.16	Ref. 15 in the text
$g\text{-C}_3\text{N}_4$	Li^+ (0.83 wt.%)	<0.20	Ref. 19 in the text
$g\text{-C}_3\text{N}_4$	Na^+ (1.20 wt.%)	0.37	Ref. 16 in the text
$g\text{-C}_3\text{N}_4$	K^+ (2.30 wt.%)	0.24	Ref. 19 in the text

Table S2 Transient emission decays of the In-g-C₃N₄ photocatalysts doped with different amount of indium.

Samples	Parameter s	Lifetime (ns)	Relative percentage (%)	Ave. τ /ns
g-C ₃ N ₄	τ_1	13.37	41.33	4.632
	τ_2	2.26	41.50	
	τ_3	90.56	17.16	
In-g-C ₃ N ₄ (0.52 wt.%)	τ_1	11.73	40.82	4.041
	τ_2	82.08	17.69	
	τ_3	1.97	41.49	
In-g-C ₃ N ₄ (1.15 wt.%)	τ_1	1.88	43.08	3.740
	τ_2	10.84	40.01	
	τ_3	75.35	16.91	
In-g-C ₃ N ₄ (2.18 wt.%)	τ_1	1.95	50.14	3.411
	τ_2	10.42	37.12	
	τ_3	82.02	12.74	
In-g-C ₃ N ₄ (2.21 wt.%)	τ_1	12.15	40.00	4.045
	τ_2	81.81	16.79	
	τ_3	2.03	43.20	